

Development of a Nanosatellite Attitude Control Simulator for Ground-based Research

Andrew Newton^a, Elyse D. Hill^b, S. Andrew Gadsden^a, and Mohammad Biglarbegian^c

^aMcMaster University, 1280 Main St. W, Hamilton, Ontario, Canada

^bNASA Glenn Research Center, 21000 Brookpark Road, Cleveland, Ohio, United States

^cUniversity of Guelph, 50 Stone Road East, Guelph, Ontario, Canada

ABSTRACT

The work presented in this paper details the design, development, and functional verification of a Nanosatellite Attitude Control Simulator (NACS). The NACS consists of a mock 1U CubeSat (MockSat), tabletop air-bearing, and automatic balancing system (ABS). The MockSat employs a reaction wheel array to exchange momentum with the rigidly attached air bearing platform, and an inertial measurement unit to obtain state estimates. The ABS tunes the center of gravity to coincidence with the center of rotation, in an attempt to minimize gravitational torques. Simulation and experimental results validate the theoretical basis of the PD controller, as well as the implementation of the numerous software and hardware modules. This experimental setup can be used by future researchers to benchmark, test, and compare different estimation and control strategies.

Keywords: Nanosatellite, Attitude Determination and Control, Spacecraft Dynamics Simulator

1. INTRODUCTION

Many spacecraft currently in orbit are subject to stringent pointing requirements in order to capture their scientific data of interest. Whether it's the James Webb Space Telescope observing the birth of stars and formation of galaxies, or a communications satellite telemetering data to a ground station, it is essential that the spacecraft can autonomously determine and control its orientation. The Attitude Determination and Control System (ADCS) is responsible for the pointing accuracy of the vehicle, thus ensuring that scientific payloads are observing their designated targets. Ground-based facilities to test and characterize the ADCS pre-launch have been employed for well over 50 years to mitigate risk and ensure quality – some examples include air bearing test beds, drop towers, and suborbital parabolic flights. The air bearing testbed has been the most widely employed solution for ADCS characterization in a simulated space environment for its ease of commissioning, access, and operation.¹⁻⁴

The earliest implementations of the air bearing Spacecraft Dynamics Simulator (SDS) correspond with the first decade of the Space Age – when spacecraft missions began to grow in complexity and the need for pointing requirements was realized. Smith¹ documents the state of the art in 1965, pointing to operational air bearing platforms at NASA's Jet Propulsion Laboratory, Ames Research Center, Langley Research Center and Marshall Space Flight Center. These original facilities were primarily employed by government and industrial entities, with payload capacities upwards of several tons. As the miniaturization of spacecraft advanced through the decades, air bearing platforms followed this trend as well, such that even a small university laboratory could own and operate an air bearing table. The review presented by Wilde et. al.³ presents a comprehensive survey of most of the air bearing simulators in academic and commercial settings, as well defines a systematic classification of air bearing simulators. This particular review was focused on the identification of planar air bearing tables, which are primarily intended for spacecraft proximity operations research and development. The review by Schwartz² is a comprehensive and well-known review of attitude dynamics simulators with three rotational degrees of freedom, and many of the systems described within form the basis for much of the design presented in this work.

Further author information: (Send correspondence to S.A.G.)

S.A.G.: E-mail: gadsdesa@mcmaster.ca

2. SYSTEM OVERVIEW

The Nanosatellite Attitude Control Simulator (NACS) consists of a mock 1U CubeSat (MockSat) and an automatically balanced hemispherical air bearing platform. The MockSat employs a Reaction Wheel Assembly (RWA) to exchange momentum with the air bearing platform, and an Inertial Measurement Unit (IMU) to obtain angular rates and orientation estimates. One rechargeable Lithium Polymer battery provides power to the actuators, and another gives power to the Raspberry Pi 3A+ control computer. All power and control signals are passed through a custom motherboard. An exploded view of the MockSat is shown below in Fig 1a.

In order to validate MockSat's attitude control abilities, a test bed was designed and built in an attempt to mimic the operating conditions of a nanosatellite in low earth orbit. The test bed is a hemispherical table-top air bearing design, which creates an extremely thin film of air to facilitate a near frictionless 3DOF joint. The air bearing provides $\pm 30^\circ$ on the pitch and roll axes, and infinite rotation about the yaw axis. An Automatic Balancing System (ABS) is currently under development, with the goal that the CoM of the fully integrated unit (MockSat and air bearing platform) can be autonomously tuned to within a 20 nm radius of the CoR. Figure 1b shows a rendering of the air bearing platform and the components of the ABS.

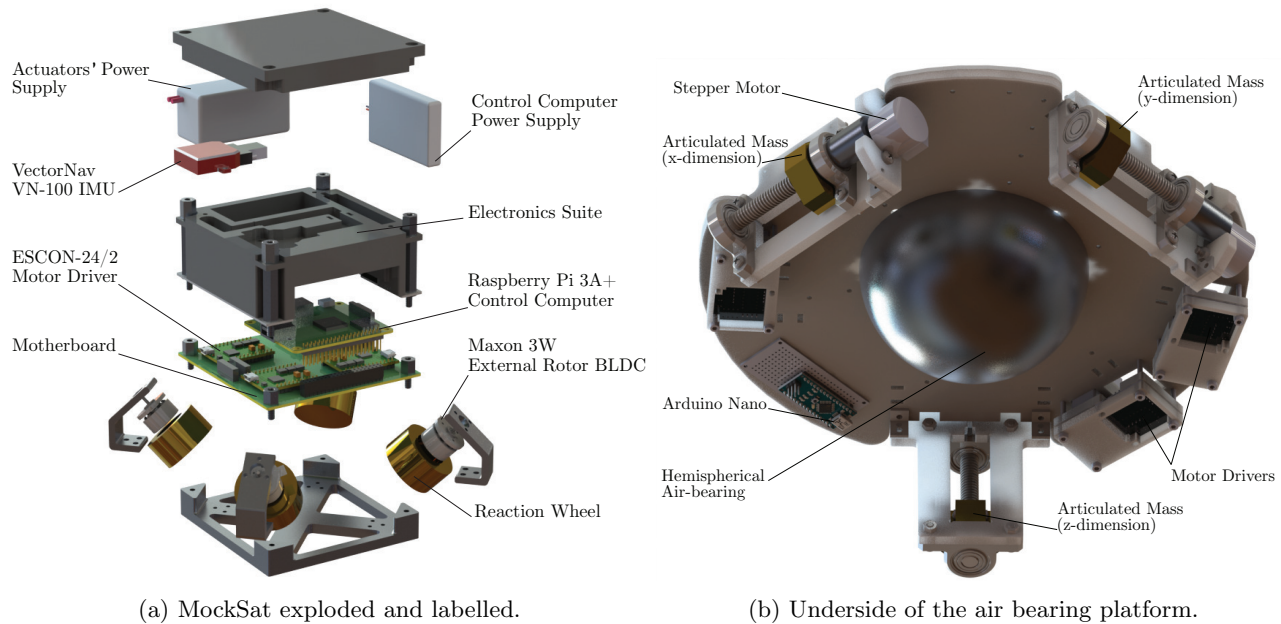


Figure 1: Main components of the NACS.

The reaction wheel assembly (RWA) contains four external-rotor brushless DC (BLDC) motors with a flywheel fixed to each of the rotors. The reaction wheel actuators were fabricated at the University of Guelph in the Physics Machine Shop. Detailed mechanical design calculations and descriptions of the manufacturing process are documented in the author's thesis.⁵ The actuators are arranged in a Pyramid configuration, although the NASA Standard configuration is another popular redundant wheel configuration, both of which are shown on the following page.

The pyramid configuration was chosen such that the Z (ie. yaw) axis of the body is given preferential control, since each reaction wheel torque vector has a component that is projected onto this axis. The yaw axis of the experimental test bed – the hemispherical air bearing – is the axis of maximum range of motion, about which the instrument can spin infinitely. As such it was desired to have preferential control about this axis. Given the desired wheel configuration, it was then necessary to specify the angle of inclination, β . This angle was taken as 45° for simplicity, as well as equal torque projection between the Z axis and X or Y axis – for example, w_1 of the pyramid configuration in Fig. 2 projects equal amounts of torque to the X and Z axes for $\beta = 45^\circ$.

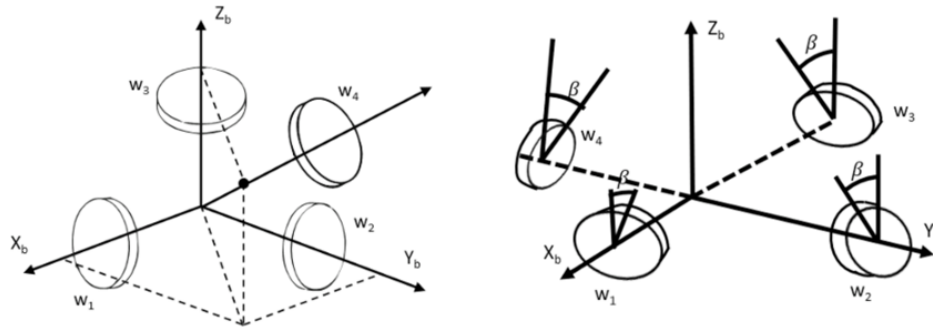


Figure 2: Left: NASA Standard Configuration, and Right: Pyramid Configuration

In summary, the NACS consists of a mock CubeSat (MockSat), and an automatically balanced air bearing table. The air bearing provides a near-frictionless 3DOF joint that supports the quasi-weightless MockSat. The ABS attempts to drive the CoG of the system to coincidence with the CoR, thereby minimizing gravitational torque disturbances. At the time of this writing, the ABS is only capable of qualitatively balancing the x and y components of the CoG, whereas the z component is manually tuned to minimize pendulous oscillations. The MockSat employs a redundantly configured RWA, which regulates the MockSat's attitude through the controlled acceleration of reaction wheels. Orientation estimates and angular rate measurements are polled from the IMU at the control loop frequency of 20Hz. A custom motherboard was designed to facilitate motor driver power and control signals, as well as the RasPi control computer. The control software is implemented in Python 3.7 – which even as a high-level interpreted language, is still capable of running the control software at 20Hz. Figure 3 shows the NACS in it's current form.

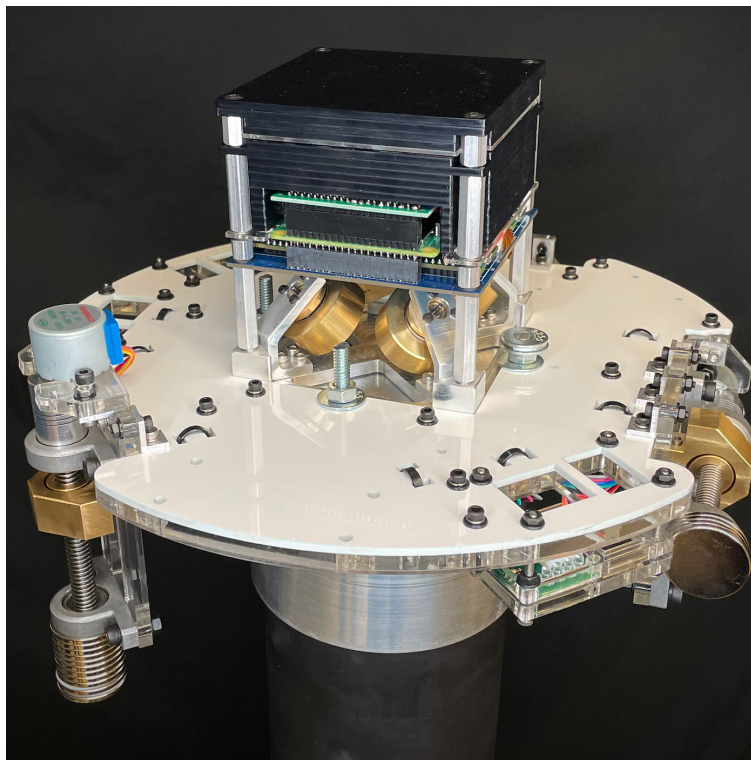


Figure 3: NACS final design.

3. MODELLING AND SIMULATION

The equations of rotational motion for a rigid body spacecraft are well documented in the literature.^{6,7} The governing equations for the NACS are derived from a kinematic and dynamic analysis, which closely follow the methods presented in.⁶

The attitude is parameterized by the quaternion, which is a computationally efficient and singularity-free description of orientation. The quaternion is a four component (redundant) description of rigid-body orientation, which expresses the spacecraft body frame $\{B\}$ relative to an fixed inertial frame $\{I\}$, denoted by \mathbf{q}_{BI} . *Euler's Theorem* asserts that "any general angular displacement between two reference frames can be accomplished by a single rotation through an angle ϑ , about an axis \mathbf{e} that is fixed in both reference frames".⁸ A quaternion that describes rotation is defined as a unit quaternion, thereby constrained to unit norm. As a result, the quaternion can be defined by

$$\mathbf{q}_{BI}(\mathbf{e}, \vartheta) = \begin{bmatrix} \mathbf{e} \sin(\vartheta/2) \\ \cos(\vartheta/2) \end{bmatrix}, \quad (1)$$

for which a rigorous mathematical proof can be found in.⁶ Equation (1) adopts the four parameter vector notation of the quaternion, such that $\mathbf{q}_{BI,1:3} = [\mathbf{e} \sin(\vartheta/2)]^T$ is the unit vector axis of rotation and $q_{BI,4} = \cos(\vartheta/2)$ is the scalar component defining the amount of rotation about \mathbf{e} . The attitude kinematic equation is derived by computing the time derivative of the attitude quaternion,

$$\dot{\mathbf{q}}_{BI} = \frac{1}{2} [\boldsymbol{\omega}_B^{BI} \otimes] \mathbf{q}_{BI}, \quad (2)$$

$$\frac{d}{dt} \begin{bmatrix} q_1 \\ q_2 \\ q_3 \\ q_4 \end{bmatrix} = \frac{1}{2} \begin{bmatrix} 0 & \omega_3 & -\omega_2 & \omega_1 \\ -\omega_3 & 0 & \omega_1 & \omega_2 \\ \omega_2 & -\omega_1 & 0 & \omega_3 \\ -\omega_1 & -\omega_2 & -\omega_3 & 0 \end{bmatrix} \begin{bmatrix} q_1 \\ q_2 \\ q_3 \\ q_4 \end{bmatrix}, \quad (3)$$

which can be acquired from the fundamental definition of the derivative, also shown in.⁶ Equation (3) requires that $\boldsymbol{\omega}_B^{BI}$ (the angular velocity matrix describing the motion of $\{B\}$ relative to $\{I\}$ expressed in $\{B\}$) is known. This is the exact purpose of the IMU, although as is the case with most sensors, noise will perturb the measurements and can lead to inaccuracies.

Given that the NACS is constrained to purely rotational motion, the dynamic equations of motion are derived through the application of Euler's Equation (the rotational analogy to Newton's Second Law). The following equation describes the dynamic motion of the MockSat. For a detailed derivation, one should consult the aforementioned reference materials.

$$\dot{\boldsymbol{\omega}}_B^{BI} = (J_B^{\text{Body}})^{-1} \left[-\mathbf{T}_B^c + [\boldsymbol{\omega}_B^{BI} \times] (J_B^{\text{Body}} \boldsymbol{\omega}_B^{BI} + W_4 (J_W^{\text{RWA}} \circ \boldsymbol{\omega}_W^{\text{RWA}})) \right]. \quad (4)$$

Equation (4) is coupled with Eq. (3) to provide a complete description of the MockSat attitude dynamics. Finally, the state-space model for the nonlinear dynamics of the NACS can be defined by

$$\dot{\mathbf{x}} = f(\mathbf{x}) + B(\mathbf{x})\mathbf{u} \quad (5)$$

where \mathbf{x} is the state vector, $\dot{\mathbf{x}}$ is the time rate of the states, and B is the control input matrix. Defining the state vector as $\mathbf{x} = [\mathbf{q}_{BI}, \boldsymbol{\omega}_B^{BI}]^T$ results in

$$\dot{\mathbf{x}} = \begin{bmatrix} \dot{\mathbf{q}}_{BI} \\ \dot{\boldsymbol{\omega}}_B^{BI} \end{bmatrix} = \begin{bmatrix} \frac{1}{2} [\boldsymbol{\omega}_B^{BI} \otimes] \mathbf{q} \\ J_B^{-1} ([\boldsymbol{\omega}_B^{BI} \times] (J_B \boldsymbol{\omega}_B^{BI} + \mathbf{H}_B^{\text{RWA}})) \end{bmatrix} + \begin{bmatrix} 0 \\ -J_B^{-1} \end{bmatrix} \mathbf{T}_B^c. \quad (6)$$

Equation (6) is used to simulate the NACS' attitude dynamics. The attitude controller is the widely accepted PD controller,

$$\mathbf{T}_B^c = -K_p \text{sgn}(q_4) \mathbf{q}_{e,1:3} - K_d (\boldsymbol{\omega}_B - \boldsymbol{\omega}_{B,d}) \quad (7)$$

for which stability has been proven through Lyapunov analysis.^{6,9} $\boldsymbol{\omega}_{B,d}$ is the desired angular rate vector of the body. K_p and K_d are gain matrices, and will determine system response characteristics like overshoot, rise time, and settling time. $\mathbf{q}_{e,1:3}$ is the vector component of the error quaternion, representing the difference between actual orientation and desired orientation. Lastly, $\text{sgn}(q_4)$ is added to ensure that the shortest route possible is taken from the current quaternion to the desired quaternion.

Simulation results for a Point-to-Point (P2P) maneuver will now be presented. The P2P maneuver is equivalent to tracking a square wave attitude setpoint signal, which may be required of a satellite when the observation target changes – a common occurrence for the Hubble Space Telescope, for example. The initial attitude is arbitrarily acquired at $\mathbf{q}(t_0) = [0.18, 0.36, 0.54, 0.73]$, corresponding to yaw-pitch-roll Euler angles of 82° , 19° , and 44° respectively. The initial angular velocity is $\boldsymbol{\omega}_B^{\text{BI}}(t_0) = [0.01, 0.01, 0.01]$. The desired attitude is a -25° slew about the yaw axis from the initial condition. The MockSat is commanded to slew to this new orientation at $t = 40\text{s}$, hold this position until $t = 80\text{s}$, then slew back to the initial condition. The desired angular velocities are zero, that is $\boldsymbol{\omega}_d = [0.0, 0.0, 0.0]$. The simulation duration is 120 seconds with a time step of 0.1 seconds. The inertia matrix of the body was approximated by a SOLIDWORKS[®] model of the NACS, given by

$$J = \begin{bmatrix} 0.020 & -0.003 & -0.001 \\ -0.003 & 0.022 & 0.001 \\ -0.001 & 0.001 & 0.029 \end{bmatrix} (\text{kg} \cdot \text{m}^2).$$

The attitude, angular rates, and control torques are plotted below.

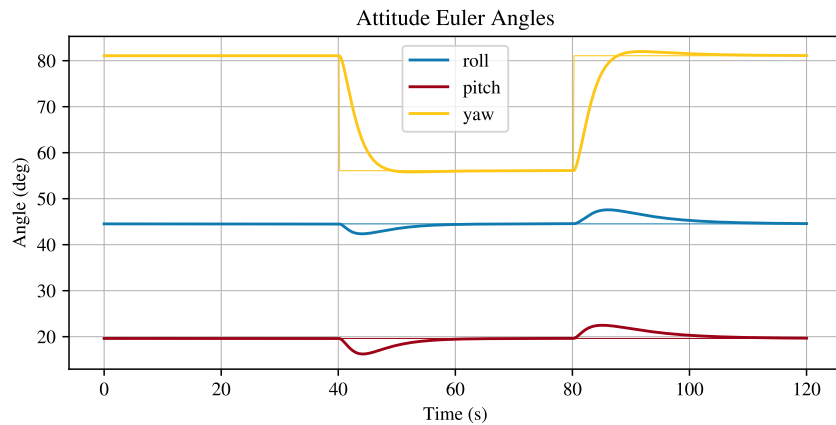


Figure 4: PD controlled Point-to-Point maneuver. $K_P = 2 \times 10^{-2}$, $K_D = 3.5 \times 10^{-2}$.

These simulation results validate the controller's ability to perform this reorientation maneuver. The first attitude setpoint is achieved in 20 seconds whereas the second reorientation is completed in 22 seconds. Only minimal overshoot is observed in the second maneuver. The accuracy performance metrics for this simulation are shown below in Table 1.

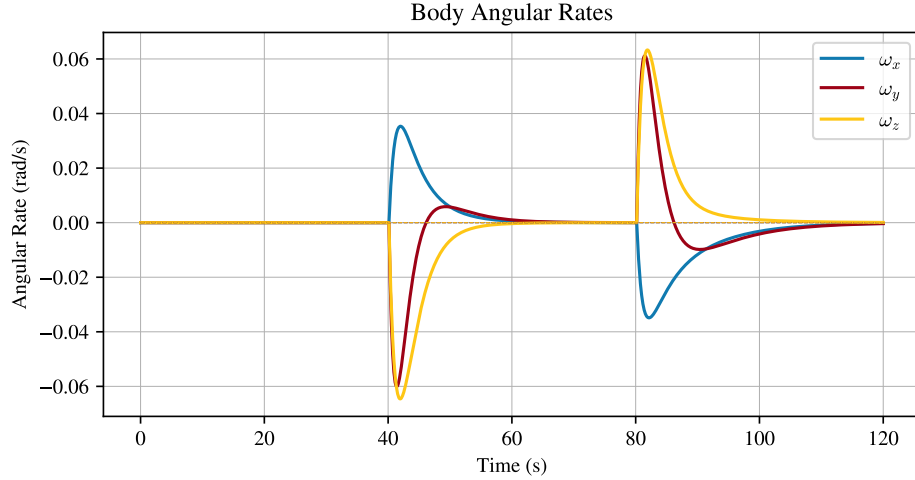


Figure 5: PD controlled Point-to-Point maneuver. $K_P = 2 \times 10^{-2}$, $K_D = 3.5 \times 10^{-2}$.

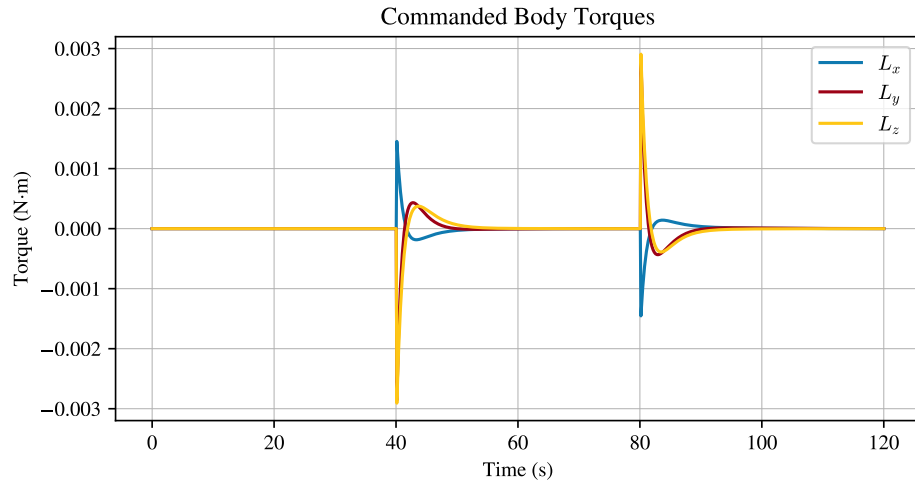


Figure 6: PD controlled Point-to-Point maneuver. $K_P = 2 \times 10^{-2}$, $K_D = 3.5 \times 10^{-2}$.

RMSE, Roll	0.96°
RMSE, Pitch	1.08°
RMSE, Yaw	4.37°
e_{ss} , Roll	0.12°
e_{ss} , Pitch	0.11°
e_{ss} , Yaw	0.07°

Table 1: Controller accuracy metrics for the P2P maneuver.

4. EXPERIMENTAL RESULTS

Experimental results will now be presented for a P2P maneuver. A multitude of experiments were conducted on the NACS in the Intelligent Control and Estimation (ICE) Laboratory at the University of Guelph in August of 2021. The purpose of these tests was to evaluate the effectiveness of a number of popular attitude controllers as well as to validate the hardware and electromechanical design of the completed device.

The following plots show the results from a PD controlled P2P maneuver. The initial quaternion was arbitrarily acquired at $\mathbf{q}_0 = [0.0, -0.03, -0.15, -0.98]^T$, corresponding to initial Euler Angles (yaw-pitch-roll) of

$[\theta_{z,0}, \theta_{y,0}, \theta_{x,0}]^T = [18.45^\circ, 3.15^\circ, 1.34^\circ]^T$. Pitch and roll initial angles are non-zero due to test bed unbalance. The initial body angular rates are zero, $\omega_0 = [0.0, 0.0, 0.0]^T$. The gains are set to $K_P = 0.65$, $K_D = 0.25$, $K_I = 0.0$. The total duration of the experiment was 120 seconds with a control loop frequency of 20 Hz. The MockSat was commanded to slew -25° about the yaw axis at $t = 40$ s, hold this position for 40 seconds, then slew back to the initial orientation. Figure 7 and 8 below chart the absolute and error attitude quaternion time histories, respectively.

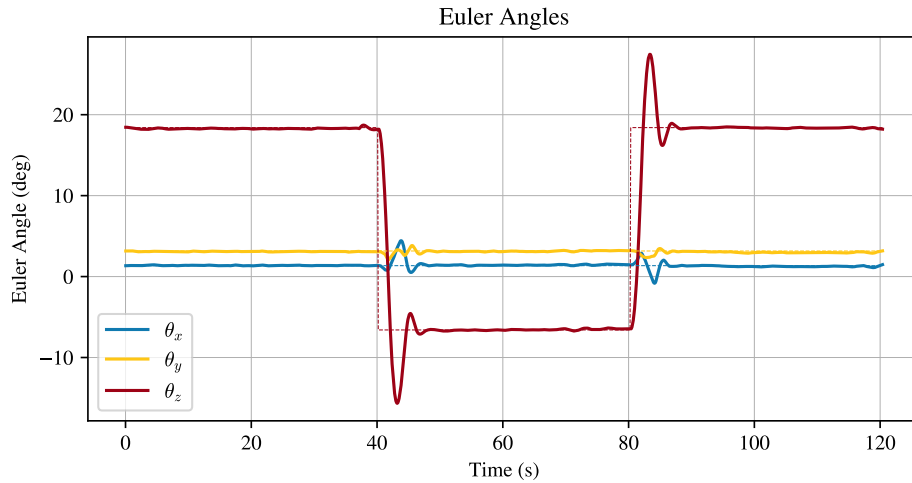


Figure 7: PID controlled P2P maneuver. Euler angles time history.

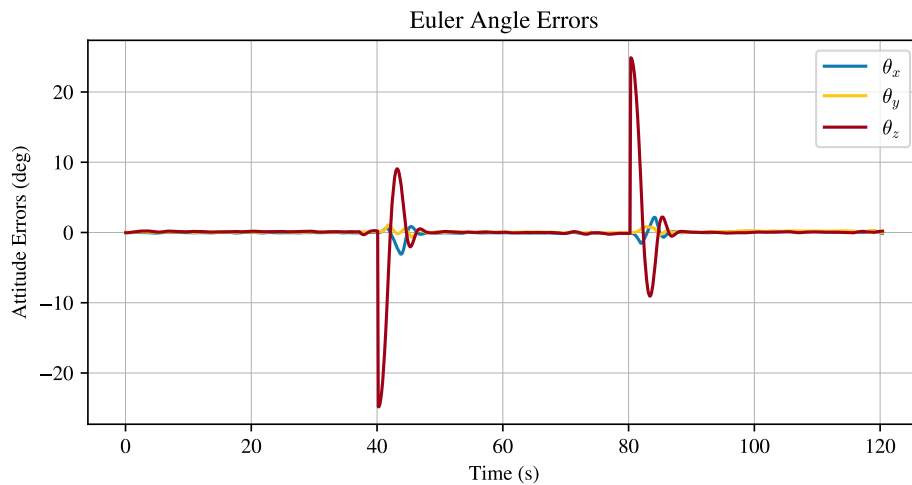


Figure 8: PID controlled P2P maneuver. Euler errors time history.

The dashed lines of Fig. 7 are the desired attitude signals. A 32% overshoot on the first reorientation is observed, followed by a 35% overshoot on its return to the initial condition. The settling time is always less than 10 seconds, and the steady-state error falls within a narrow 0.5° tolerance band. The most exciting artifact of the data is the Euler error time history, which shows a near perfect attitude solution for the entire experiment, except for the instances at which a reorientation maneuver begins. Figures 9 and 10 below show the commanded body torques output from the controller (T_B^c) and the resulting body angular rates.

Figure 9 charts the commanded control torques as seen in the body frame, and the resulting body angular rates are shown in Fig. 10. Control torques are always non-zero to correct for the aerodynamic disturbance

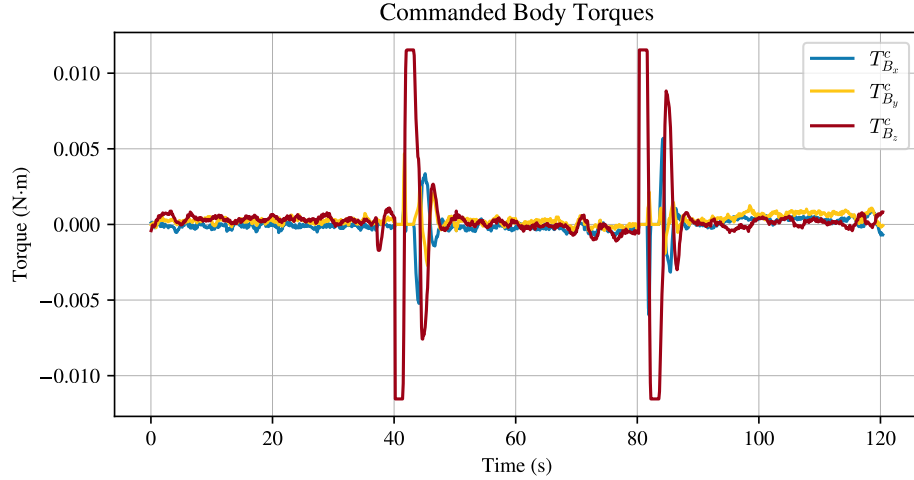


Figure 9: PID controlled P2P maneuver. Corrective body frame torques.

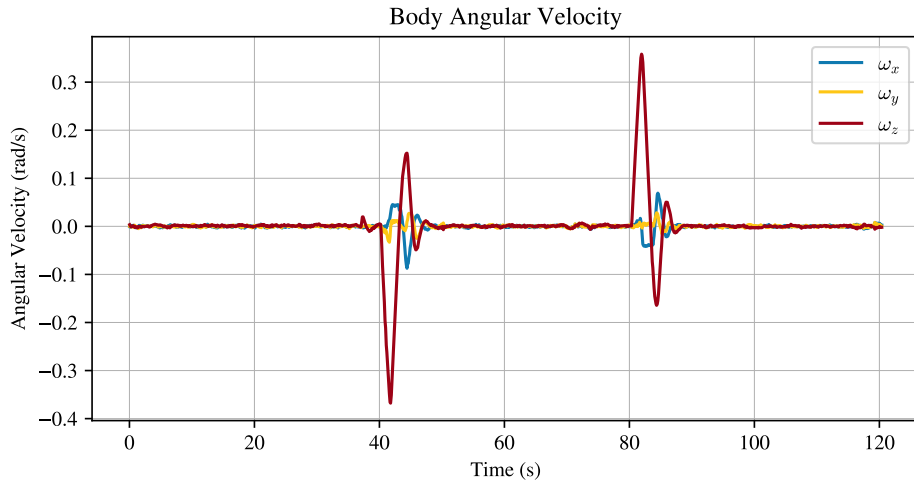


Figure 10: PID controlled P2P maneuver. Body Angular rates.

torque applied by the air-bearing. At $t = 40s$, the control signal is immediately saturated which indicates that the K_P control gain can be lowered without compromising the system response. In fact this would decrease the percent overshoot at the cost of an increased rise-time. Alternatively, one could adjust the k_D gain term, which is intuitively understood as the damping term. Table 2 below consolidates the performance metrics from the P2P test. The Root Mean Square Error (RMSE) of the Euler angles and the steady-state error (e_{ss}) are strong indicators of pointing accuracy.

RMSE, θ_x	0.39°
RMSE, θ_y	0.18°
RMSE, θ_z	3.54°
e_{ss} , θ_x	0.09°
e_{ss} , θ_y	0.18°
e_{ss} , θ_z	0.05°

Table 2: NACS attitude accuracy metrics for the P2P maneuver.

5. CONCLUSION

This work briefly presented the design, development, and experimental validation of a nanosatellite attitude control simulator. The simulator consists of a MockSat, air-bearing table, and automatic balancing system. The software is completely implemented in Python 3.7, which streamlines software development and allows a researcher to focus on theory rather than syntax.

The NACS has demonstrated its value as a reliable and interesting tool for the collection of experimental data, serving as a test-bed for research on model predictive control strategies for fault tolerance.¹⁰ This work touched mainly on the design and development of the instrument, but the potential applications for research are extensive. The author's first recommendation is to use the ABS in concert with the ADCS in a system identification campaign. The input/output characteristics of the system can be measured by the motor controllers and IMU, and then passed to a predictive algorithm to accurately determine the inertia matrix. This would allow for increased accuracy in the application of model based controllers, such as the model predictive controller. This instrument could also be used in the validation of estimation algorithms. Currently, the IMU estimates the orientation on-board, based on the models of the internal MEMS sensors. However, raw data can be polled from the sensor instead and passed to estimation algorithms running on the Raspberry Pi and based on the system dynamics model defined by Eqs. 3 and 4. Lastly, the author recommends that the NACS's range of motion should be extended to $\pm 360^\circ$ about all axes. This can be accomplished by housing the MockSat within a "hamster ball" of sorts, which is then seated on the air cushion. This would allow for a true characterization of the ability in performing orbit-like maneuvers.

REFERENCES

- [1] Smith, G., "Dynamic simulators for test of space vehicle attitude control systems," tech. rep., NASA Langley Research Center (1965). Accessed: 2021-02-25.
- [2] Schwartz, J., Peck, M., and Hall, C., "Historical review of air-bearing spacecraft simulators," *Journal of Guidance, Control, and Dynamics* **26** (05 2003).
- [3] Wilde, M., Clark, C., and Romano, M., "Historical survey of kinematic and dynamic spacecraft simulators for laboratory experimentation of on-orbit proximity maneuvers," *Progress in Aerospace Sciences* **110** (08 2019).
- [4] Gavrilovich, I., *Development of a robotic system for cubesat attitude determination and control system ground tests.*, PhD thesis, Universite Montpellier (2016). English. NNT:2016MONTT329. tel-01816985.
- [5] Newton, A., *Design, Development, and Experimental Validation of a Nanosatellite Attitude Control Simulator*, Master's thesis, University of Guelph (2021).
- [6] Markley, F. L. and Crassidis, J. L., [*Fundamentals of Spacecraft Attitude Determination and Control*], Springer (2014).
- [7] Wertz, J. R., [*Spacecraft Attitude Determination and Control*], Springer (1978).
- [8] Tsiotras, P. and Longuski, J. M., "A new parameterization of the attitude kinematics," *The Journal of the Astronautical Sciences* **43**(3) (1995).
- [9] Wie, B. and Barba, P., "Quaternion feedback for spacecraft large angle maneuvers," in [*Journal of Guidance, Control, and Dynamics*], 360-365 (1985).
- [10] Hill, E., *Model Predictive Control Strategies for Fault Tolerance*, PhD thesis, University of Guelph (2021).